Imaging electric and magnetic orders using scanning probe microscopy

Sandra Sajan

A dissertation submitted for the partial fulfillment of
BS-MS dual degree in Science

Indian Institute of Science Education and Research Mohali

May 2020

Certificate of Examination

This is to certify that the dissertation titled "**Imaging electric and magnetic orders using scanning probe microscopy** " submitted by **Ms. Sandra Sajan** (Reg. No. MS15088) for the partial fulfillment of BS-MS dual degree program of the Institute, has been examined by the thesis committee duly appointed by the Institute. The committee finds the work done by the candidate satisfactory and recommends that the report be accepted.

Dr. Abhishek Chaudhuri Dr. Sanjeev Kumar Dr. Goutam Sheet
(Supervisor)

Dated: May 4, 2020

Declaration

The work presented in this dissertation has been carried out by me under guidance of Dr. Goutam Sheet at the Indian Institute of Science Education and Research Mohali.

This work has not been submitted in part or in full for a degree, a diploma, or a fellowship to any other university or institute. Whenever contributions of others are involved, every effort is made to indicate this clearly, with due acknowledgement of collaborative research and discussions. This thesis is a bonafide record of original work done by me and all sources listed within have been detailed in the bibliography.

Sandra Sajan

(Candidate)

Dated: May 4, 2020

In my capacity as the supervisor of the candidate's project work, I certify that the above statements by the candidate are true to the best of my knowledge.

Dr. Goutam Sheet
(Supervisor)

Acknowledgements

Foremost, I would like to express my sincere gratitude to my advisor and research guide $Dr.GoutamSheet$ for allowing me to research under his guidance and for providing me with constant encouragement and support. His immense knowledge, dedication and motivation have helped me throughout the research. My work would have been incomplete without his support and pieces of advice.

I would also like to thank my thesis committee members for their valuable suggestions and feedback.

I am grateful to *Ranjani*, *Nikhil* and *Monika* for their involvement, technical support and for all the time we spend together in the AFM lab. I also thank my all other fellow labmates in SPIN LAB GROUP: *Aastha, Deepthi, Mona, Nikhlesh, Ritesh, Sandeep, Shivam, Soumyadatta, Soumyadip and Veerpal* for all timely advice and help. All of them were compassionate and considerate enough to dedicate their time whenever I asked them for any help. I am also indebted to *Dr.Kanishka Biswas* and *Debattam Sarkar* for providing me $AgBiSe_2$ sample and *Dr.Pintu Das* for providing me with hall bar sample.

I thank all my friends in IISER for all the love and joy we shared each other. I will always cherish those memories. I will never forget your willingness to help me even when not asked. I am always grateful to you: *Ashitha, Aiswarya, Farsana, Fidha, Nihal, Ramsi, Sumith*.

Last but not the least, I would like to thank my family, my father, mother and brother for providing constant encouragement and for supporting me both spiritually and mentally. You have never forgotten to bring a smile on my face even in toughest times.

List of Figures

Abbreviations

um	**m**icro **m**eter
pm	pico meter
nm	nano meter
laser	**l**ight **a**mplification by **s**timulated **e**mission of **r**adiation
PZT	Piezo electric actuator
AFM	Atomic force microscopy
SEM	Scanning electron microscope
MFM	Magnetic force microscopy
PFM	Peizoresponse force microscopy

Contents

Dedicated to my parents and brother

Abstract

In this thesis, we employ different scanning probe microscopic techniques to probe electric and magnetic orders in different samples. In the first chapter, we try to examine the principles and components of atomic force microscopy. This involves exploring the hardware components and modes of operation involved in the AFM technique.

In the next chapter, we employ Piezoresponse force microscopy to study local ferroelectric polarization in rhombohedral p-type GeSe crystal, which is a thermoelectric material. The thermoelectric performance of this sample is induced by ferroelectric instability in the material. Here we show the presence of local ferroelectricity in this material by imaging ferroelectric domains and performing switching spectroscopy PFM.

In the third chapter, we try to image magnetic orders in two different materials namely, a Co/Pt/Fe hall bar device and Fe_2O_3 nanoparticles by performing magnetic force microscopy. The ability of MFM to image these samples at very high resolution have a wide variety of application in storage, logic computing gates, non conventional devices, and different biological applications.

In the final chapter, we try to image artificial spin ice using magnetic force microscopy. Artificial spin ice consists of complex nanosized arrays of ferromagnetic islands arranged on specific lattice fabricated using lithographic techniques. It has enabled the experimental investigation of a variety of fascinating phenomena such as frustration, disorder, and phase transitions. Here we look at fabrication and imaging of these artificial spin ice material which has enormous future research prospects.

Chapter 1

Atomic force microscopy

1.1 Introduction

Atomic force microscopy is a type of scanning probe microscopy technique which can probe the surface of the order of nanoscale. It is employed in various chemical, biological, and physical research field for measuring, maintaining and manipulating the local properties of the material such as height, magnetisation etc. AFM measurements are mostly based on the force-distance curve, where a probe is moved vertically along the surface of the sample and force applied between the probe and the sample is measured as a function of distance moved by the probe by plotting force-distance curve. For imaging, the surface, height of the sample is measured and recorded as a function of probe sample interaction by scanning over the surface of the sample. Techniques such as scanning probe lithography are used in manipulation where sample properties can be varied and controlled by adjusting the force between the sample and the probe[Yongho Seo, 2008].

AFM operates by using a probe called cantilever which measures the force between the tip and sample surface. Detection of cantilever movement is achieved by various techniques which include optical deflection, tunnelling current measurement, fibre interferometry etc. An earlier model of AFM was developed by Binning in 1986 16. He attached a diamond tip to an optical lever made up the gold foil. Optical lever was driven at its resonance frequency simultaneously maintaining constant force between the tip and sample. The vertical movement was detected by placing an STM tip above the cantilever. Now mostly Si and Si_3N4

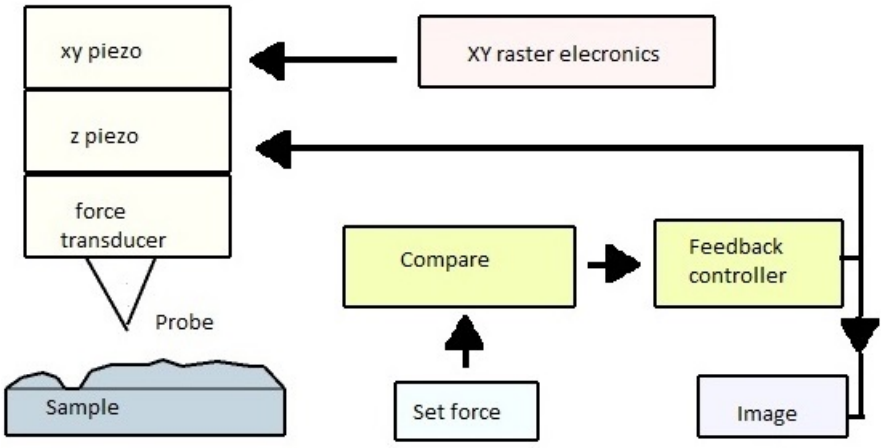

FIGURE 1.1: Block diagram of AFM operation

cantilevers are usually employed which has a reflective coating for optical deflection. With recent developments, many properties including the friction, electrical force, capacitance, magnetic force, viscoelasticity can be measured using an AFM.

1.2 Principles of Atomic force microscopy

AFM allows us to image the surfaces of conductors and insulators with atomic resolution. The most widely used technique for atomic force microscopy was first developed by Amer and Meyer which involves a tip, usually made up of Si or Si_2N_3 mounted on a cantilever. As the tip is scanned across the surface of the sample, the interatomic attractive forces between the tip and the surface causes the tip to get deflected towards the surface. As the tip goes closer to the surface it gets deflected away from the surface due to repulsive forces. A laser beam is used to detect the deflections of the cantilever. An incident laser beam is allowed to fall on the flat cantilever surface which gets reflected off in slightly different direction due to cantilever deflections. A position-sensitive photodiode is used to track the laser direction and records the topography of the sample as the cantilever gets deflected which sends the signal to a lock-in amplifier. A feedback loop is used to maintain a constant height between the sample and the tip which maintains a constant set point. The control signal from the lock-in amplifier is then used to generate the image[Nabil Mahmoud Amer, 1992].

The most commonly used modes in AFM are contact, non-contact and tapping modes. In contact mode, the tip scans across the surface of the sample in continuous close contact. Here the force between the tip and the sample is repulsive. It can operate in mainly two configurations which are constant deflection mode or constant height mode. In constant deflection mode, a DC feedback amplifier measures the deflection of the cantilever and compares it with a constant value of deflection. If the deflection is different from the set value it applies a voltage to the piezo which then tries to adjust the cantilever to maintain constant deflection. The voltage that is applied by the piezo is measured and recorded as the height of the sample surface. In constant height mode, the probe maintains a constant height above the sample and there is no force feedback in this method. The non-contact mode is used in samples where the sample surface can get altered by the tip. Here the force between the tip and the sample is attractive Van der Waals force which is generally weaker. Hence an oscillating AC signal is applied to the tip which then measures the change in amplitude, phase or frequency of oscillation in response to change in interaction strength. This is then recorded to obtain the surface topography. The tapping mode offers an advantage over the contact and non-contact mode that it has sufficient oscillation amplitude to avoid any tip-sample adhesion which can cause damage during the scan and provide enough signal strength for high-resolution imaging. In tapping mode, the tip is given an oscillation near its resonance frequency. As the tip scans across the surface it is alternatively placed in contact with the surface and then lifted off. Due to tip-sample interaction, the oscillation amplitude is greatly reduced when the tip is in contact with the sample, which is then used to measure any change in the sample surface.

1.3 Tip sample interaction

The force between the tip and the sample can be classified into both attractive and repulsive forces. The repulsive forces are generally short-ranged and have inverse square law dependence with distance. The attractive force between the sample and tip includes Van der Waals force, electrostatic force, chemical force, capillary forces etc. Let us consider the Lennard-Jones potential for atomic interaction between two atoms[Giessibl, 2003].

$$U(r) = 4\epsilon\left[-\frac{\sigma^6}{z^6} + \frac{\sigma^{12}}{z^{12}}\right] \tag{1.1}$$

where is an interaction parameter, z is the distance between the tip and the sample, and ϵ is the depth of the potential well. The first term is the Van der Waals term and the second term characterizes the repulsive forces. For many-body interaction between the tip and sample, Hamaker's approach could be used for sample and tip of radius less than 10 nm. For a spherical tip with radius R and a flat sample, the VdW potential V_{vdW} is given by

$$V_{VdW} = \frac{A_H R}{6z} \tag{1.2}$$

where z is the closest distance between the tip and the sample and A_H is the Hamaker constant. Hence the force between the spherical tip and sample is of order z^{-2} while for cylindrical and pyramidal tips it is Z^{-2}. VdW force provides a major contribution to AFM measurements due to its large magnitude. Another major interaction is the electrostatic interaction between the tip and sample which is conductive. For a tip and sample with potential difference U and separated by distance d, the electrostatic force is given by

$$F_e l(z) = \frac{\epsilon_0 R U^2}{z} \tag{1.3}$$

where R is the tip radius and ϵ is the dielectric constant. The electrostatic force is long-ranged compared to the VdW force. Chemical forces between the sample and tip can also be a major factor that determines the interaction between them. The Morse potential

$$V_{Morse} = E_{bond}(2e^{\kappa(z-\sigma)} - e^{2\kappa(z-\sigma)}), \tag{1.4}$$

can be used to describe the chemical bond with bonding energy E_bond, equilibrium distance s, and a decay length k. The chemical force is generally short ranged force. The repulsive interaction originating from Coulomb force or Pauli exclusion is also short-ranged. In Lennard Jones potential given in equation(1.1), the second term describes the repulsive force between the tip and the sample[Yongho Seo, 2008].

1.4 Components of AFM

There are mainly three basic concepts in AFM instrumentation. They are piezoelectric transducers, force sensors and feedback control. Piezoelectric transducers(PZT) moves the tip and sample while feedback control tries to maintain a constant force between the tip and sample by sending a signal from the force sensor to piezo actuators. PZT is based on

the principle of piezoelectric effect where mechanical stress or force applied along certain directions produce electric charges on the material. The rate of mechanical stress is directly proportional to the rate of the electric charge produced. Piezoelectric material used in the AFM is mostly synthetic ceramic materials. By applying a voltage across the surface of Piezoelectric transducers, it changes geometry in the range of atomic scale. Hence they can be used to control the motion of the probe while scanning as well as the scanner and other parts which require fine movement. Force transducers in an AFM consists of a tip mounted on a cantilever and optical lever. They measure the force between the AFM probe and the sample surface. The signal from the force sensor is sent to feedback control which will then try to maintain a constant force between sample and tip. This is done by controlling the piezoelectric components associated with the motion of cantilever and the tip.

1.4.1 Hardware components

The major hardware component in an AFM is an AFM stage which includes the probe, sample holders, coarse approach system and X-Y-Z positioning system. To approach the surface, it also contains an optical microscope to see the sample and tip. The whole stage is in a set up where it is isolated from any vibrations or external forces. There are mainly two types of scanning configurations; the samples scanning AFM where the sample is moved relative to a fixed probe while scanning and a probe scanning AFM where the probe is moved. Most commercial AFMs use sample scanning technique because it is easier to construct[Peter Eaton, 2010].

1.4.1.1 Scanners

The scanners used in an AFM are made up of piezoelectric material like barium titanate or led zirconium titanate. This piezoelectric material can be fabricated in different shape and configuration to control the motion. While a disc shape gets longer and narrower when applied voltage a bimorph configuration changes the shape in a parabolic way with all of them preserving the volume. The piezoelectric material is expected to change the shape in proportion to the applied voltage. The X-Y axis moves in a raster pattern and the motion of the z-axis which is vertical is controlled by the signals from the feedback controller.
In a real system, the piezoelectric material shows nonlinear behaviour like hysteresis where it tries to maintain the shape. Sometimes it can behave in such a way that it continues

its motion even after the applied voltage has been stopped. This behaviour is usually corrected using an open or a closed-loop method[Jagmeet S Sekhon and Sheet, 2014]. In an open-loop technique image is corrected after measuring the position of the scanner while in closed-loop technique motion of the probe is corrected in real-time with feedback electronic circuit. Both of this technique requires calibration using a known sample which will be scanned for measuring non-linearities. For correction, it is also important to detect the position of Piezo scanners. This is done with the help of displacement sensors which includes light-based sensors, capacitance sensors, inductance sensors, strain gauges etc. The most common are capacitance sensors which measure the movement of the scanner by measuring capacitance which depends on the distance between plates. Sometimes an inductance sensor is also useful which measures the strength of electromagnetic coupling between the sensor and target. In an open-loop configuration, it can be difficult to zoom from higher scan size to a lower and vice versa. Hence closed-loop configuration is mostly employed with calibration sensors where it can do both correction and zooming. The Z-axis also involves the Piezoelectric scanner in a correction mechanism in an open-loop configuration. The closed-loop configuration cannot be applied here because scanner motion is unpredictable. AFM techniques some times take the z-sensor signals for accurate measurements. Three basic design in an AFM scanner is tube, tripod, and flexure scanners. The tube scanners which are in the shape of tube or cylinder can move X, Y and Z axis while a flexure scanner involves pushing on a flexure with a piezoelectric element.

1.4.1.2 Force sensors

The force sensor measures the force between tip and sample surface which gives information of sample topography. The most widely used sensor is an optical level sensor. It consists of a laser beam which is made to fall on the reflecting side of the cantilever. When the tip scans across the surface, the interaction between the tip and sample changes the path of the reflected beam. To measure the force change in laser, the position is detected by four quadrants of a laser. One mechanism consists of a laser and photodetector scanning in the X-Y axis and probe moving in the Z-axis. Here X-Y scanner consists of a flexure scanner that changes light path as Z scanner made up of piezo stock is moved up and down.

1.4.1.3 Coarse X-Y-Z movement

Coarse Z movement is required for the tip to approach the sample surface without crashing the tip and sample. There are generally two mechanisms involved in approaching the samples. One is a stepper motor approach which is driven by 80 turns per inch screw or a linear bearing and other is Z piezoelectric scanner. The feedback mechanism allows detecting whether the Probe has reached the sample. One of the simple mechanism to control Z motion involves three lead screws mounted on a fixed structure. Very fine movement can be created if only one of the screw is turned. Depending on the number of screws turned we can control the motion. Another simple mechanism involves the use of linear bearing. The X-Y positioning stage for AFM involves manual or automated stages that could locate the area on the sample.

1.4.2 Feed Back mechanism

To maintain a constant force between the tip and the sample, a feedback mechanism is used. It takes the signal from the force sensor, compares it with setpoint values and the error signal is then sent to a feedback controller which drives z piezo element. The signal from the force sensor is different for both contact and non-contact mode. For contact mode, the signal is the deflection of cantilever while for non-contact mode it is oscillation amplitude. The feedback controller in AFM is called a proportional integral derivative controller(PID). It is governed by the equation,

$$Z_v = P \times V_{error} + I \times \int Z_{error} dt + D \times \frac{dZ_{error}}{dt} \tag{1.5}$$

where Z_v is the voltage which is converted to height or topography. Here P, I, D values are selected to scan the instrument across the surface making Z_{error} very small. The integral term allows the surface to follow large surface features while proportional and derivative term allows the instrument to follow small surface feature. However, the most commonly used AFMs only have PI controllers. In the process of optimising the PID parameters, the error is minimised. Another important factor in feedback mechanism is the scan rate and set point. Faster scan rate can give wrong data since it gives less time for the PID controller to send the signal to adjust it back to set point. Feed back can get slower by taking a set point closest to the out of contact feedback.

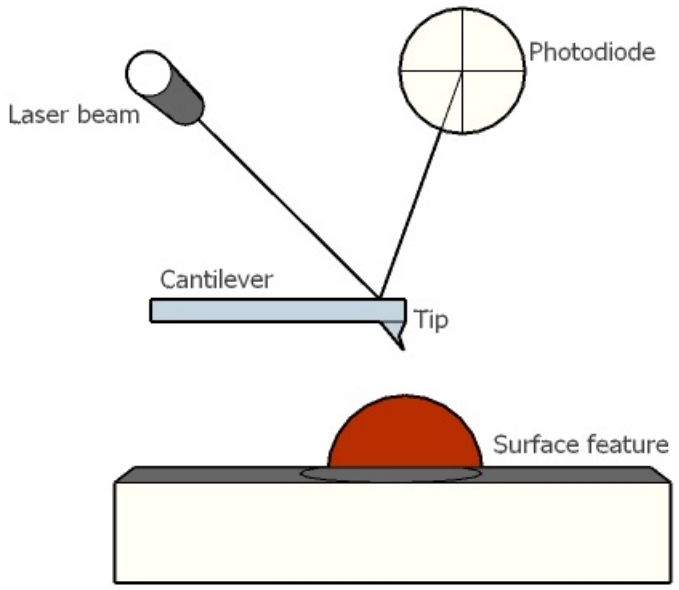

FIGURE 1.2: Schematic of optical lever detection method

1.4.3 AFM Cantilever

The probe used in AFM involves a tip which is mounted on a cantilever. This is usually a disposable component of AFM. The shape and material of the cantilever tip are important in both the quality and mode of the scan. The two commonly used material for contact mode AFM is Silicon and Silicon Nitride which has a spring constant of less than 1N/m. They are called soft cantilevers. In an oscillating mode, the material is mostly Si and has much greater spring constants of 10N/m or more and hence called stiff cantilevers. Such cantilevers allows maximum scanning speed in measurements. The spring constant K varies with cantilever dimension as,

$$k = \frac{Ywt^3}{4L^3} \tag{1.6}$$

where w is the cantilever width, t is the cantilever thickness; L is cantilever length and Y is Young's modulus of the cantilever material. Usually, the cantilever has a radius of curvature of about 5-10 nm. They are mostly found in rectangular and triangular geometries. To perform the measurements the cantilevers needed to be calibrated for force constants. The most commonly used method for calibration constants is the Sader method where the physical dimensions of the cantilever, as well as the quality factor, is measured to calculate the spring constant.

1.5 Advanced Imaging Methods

Additional imaging modes can be used to perform measurements on the sample to explore electric and magnetic properties. The method involves distinguishing the corresponding force from VdW force by usually employing a lifting mechanism. The lifting is done in either a single pass or dual pass mode. In single-pass mode, after performing a full topography scan on the sample, the probe is lifted to a certain height and the forces are measured again. In dual-pass mode, the topography is scanned in the forward pass and in the backward pass, the tip is lifted and the difference is recorded to obtain the forces. In dual-pass mode hence topography and other interactions can be scanned simultaneously.

Chapter 2

Local ferroelectricity in rhombohedral p-type GeSe crystal

2.1 Introduction

Thermoelectric materials convert heat into electricity based on Seebeck and Peltier effect. They are characterised by high electrical conductivity and low thermal conductivity. There is ongoing research for new materials with high thermoelectric efficiency that involve abundant and environment-friendly materials. The rhombohedral phase of GeSe has recently attracted attention due to the theoretical prediction of high thermoelectric figure of merit. However, the experimental values of thermoelectric performance were low due to low carrier concentration. It was shown experimentally that cubic GeSe stabilised by alloying with $AgBiSe_2$ showed high thermoelectric performance[Roychowdhury, 2017]. Rhombohedral GeSe has shown low thermal conductivity and high thermoelectric performance by doping it with $AgBiSe_2$[Huang, 2017]. By investigating the ferroelectric nature of the material, it was reported that high thermoelectric performance and low thermal conductivity have been caused by the presence of ferroelectric instability. Here I will try to discuss the existence of local ferroelectricity in $AgBiSe_2$ and $AgBiTe_2$ doped GeSe.

Here we employ Piezoresponse force microscopy to image the ferroelectric domains in both rhombohedral $(GeSe)_x(AgBiSe_2)_{1-x}$ and $(GeSe)_x(AgBiTe_2)_{1-x}$. PFM is used to directly show local polarization switching in the materials, indicating ferroelectric behaviour,

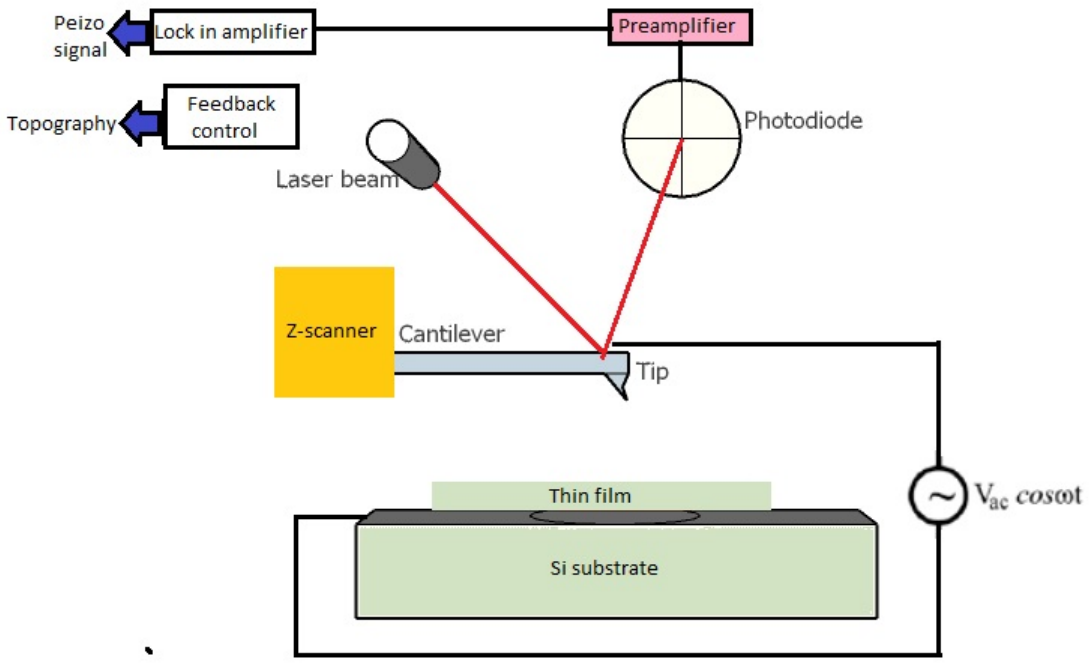

FIGURE 2.1: Schematic of PFM set up

although global ferroelectric ordering has not been observed. We also observe clear butterfly loops in local strain vs DC voltage which is a clear indication of ferroelectricity. The observed ferroelectric behaviour supports the previous observation of low thermal conductivity and high thermoelectric performance in this material induced by the ferroelectric instability.

2.2 Overview

PFM measures the mechanical response of the sample surface in response to the applied electric signal. Here a conductive cantilever is scanned across the surface of the sample in contact mode. An AC bias is applied to the tip while scanning. There is periodic deflection in the cantilever due to deformation in the sample caused by an electric field. The electromechanical response can also be probed as a function of DC Bias which provides information on polarisation switching in ferroelectric materials[Proksch and Kalinin,]. Here the voltage is applied to the conductive tip as

$$V_{tip} = V_{DC} + V_{AC}cos(\omega t) \tag{2.1}$$

Where V_{DC} is the DC bias and $V_{cos(\omega t)}$ is the AC bias. Due to the converse piezoelectric effect, the sample gets deformed which is monitored by a lock-in amplifier which gives tip oscillations of the form

$$A = A_0 + zcos(\omega t + \phi) \tag{2.2}$$

where A_0 is the static surface displacement and ϕ is the phase shift between the driving voltage z is the resulting piezoelectric strain in the material that causes cantilever displacement.

$$z = d_{33}V_{DC} + d_{33}V_{AC}cos(\omega t + \phi) \tag{2.3}$$

where the first term is due to local piezoelectric deformation and the second term is due to local electrostatic deformation caused by both local and non-local Maxwell stress. If the polarization of the sample is parallel to the applied electric field, the piezo effect will be positive and the sample will expand. If the local sample polarisation is anti-parallel with the applied electric field the sample will shrink. Hence the phase of polarisation can be used to polarisation orientation of the sample when an oscillating voltage is applied. PFM amplitude data gives information on the magnitude of local electromagnetic coupling.

2.2.1 DART PFM

In PFM, an AC bias is applied to the sample which can lead to sample deformations. Hence the contact resonance will be dependent on the elastic modulus of the material which can vary along the sample surface. This results in topographic cross talks due to the shift in resonance frequency along the sample surface. ”Dual AC resonance tracking ” is an imaging technique which used to reduce the cross-talk using a feedback loop and adjusting the drive frequency of the cantilever to match the resonant frequency. Two oscillating frequencies near-resonant frequency is supplied to the cantilever which uses the difference between two amplitudes as the input feedback. The two oscillating frequencies are chosen in such a way that one lies above resonant frequency and one lies below it. Let A1 and A2 be two resultant amplitude when the resonant frequency shifts, then if the frequency shifts downward A1 moves up to A1 and A2 moves down to A2. This change causes the feedback loop to shift the drive frequencies until the difference is zero.

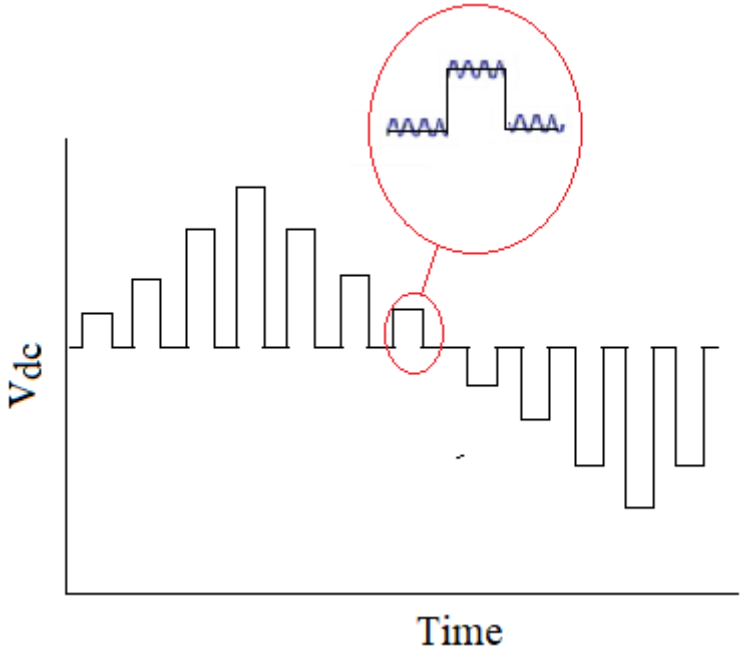

FIGURE 2.2: Combination of AC and DC signal in triangular saw tooth form for PFM spectroscopy

2.2.2 PFM Spectroscopy

PFM spectroscopy involves generating hysteresis loops in ferroelectric materials which can give information about local ferroelectricity in the materials. In PFM spectroscopy a conducting cantilever is bought in contact with the sample and the electromechanical response of the sample as a function of the applied DC bias is measured. A varying AC field is applied along with varying DC field. Here we use Switching spectroscopy mapping techniques for studying the ferroelectric switching. This involves a square wave which carries a sine wave and takes magnitude in the form of steps. The DC bias offset is made zero between each increasing voltage step to determine any bias induced changes in the material. The response signal is taken mainly in the form of phase and the amplitude. A hysteresis in-phase and the phase switching of 180 with applied DC bias is used in confirming the presence of ferroelectricity in the material. The Butterfly loop in the amplitude vs. DC bias is yet another signature of ferroelectricity.

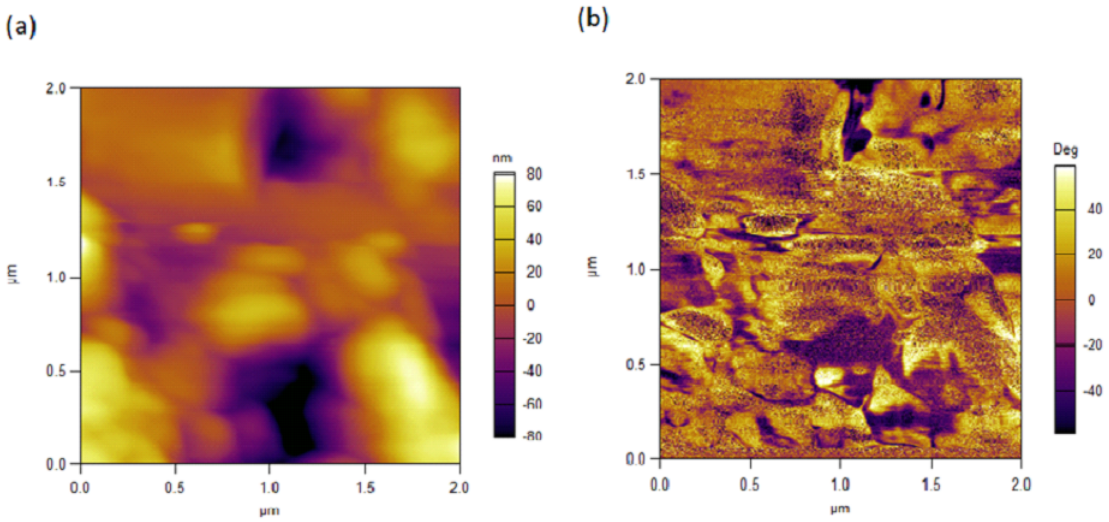

FIGURE 2.3: Topography and phase image for $AgBiSe_2$($2\mu m \times 2\mu m$)

2.3 Results

To perform PFM measurements, a conducting cantilever, made of silicon coated with Platinum, was brought in contact with both $AgBiSe_2$ alloyed GeSe and $AgBiTe_2$ alloyed GeSe. An excitation voltage of 3V was applied to the cantilever and the amplitude response function of the cantilever was recorded as a function of frequency to obtain contact resonance. The free air resonant frequency was found to be around 70 kHz for both the samples. The resonant frequency in contact with the samples was found to vary between 290 - 330 kHz. The spring constant of the cantilever was found to be 2.1 N/m. To examine ferroelectric behaviour, we carried out piezoresponse force microscopic imaging in $AgBiSe_2$ and $AgBiTe_2$ doped GeSe. Imaging was performed in contact mode using DART techniques. For this purpose, an AC voltage was applied between the tip and the sample and the response signal was recorded. The magnitude of phase is then plotted as a function of the position of the tip which gave an image which displays the distribution of ferroelectric domains in the sample. Here the topographic and phase image evidence the presence of local ferroelectric domains with uniform electrical polarization. The bright and dark contrast in the phase image of both the samples(Fig 2.4, Fig 2.5) indicates the presence of oppositely polarised neighbouring domains.

To further ascertain the ferroelectric behaviour we investigated the presence of spontaneous

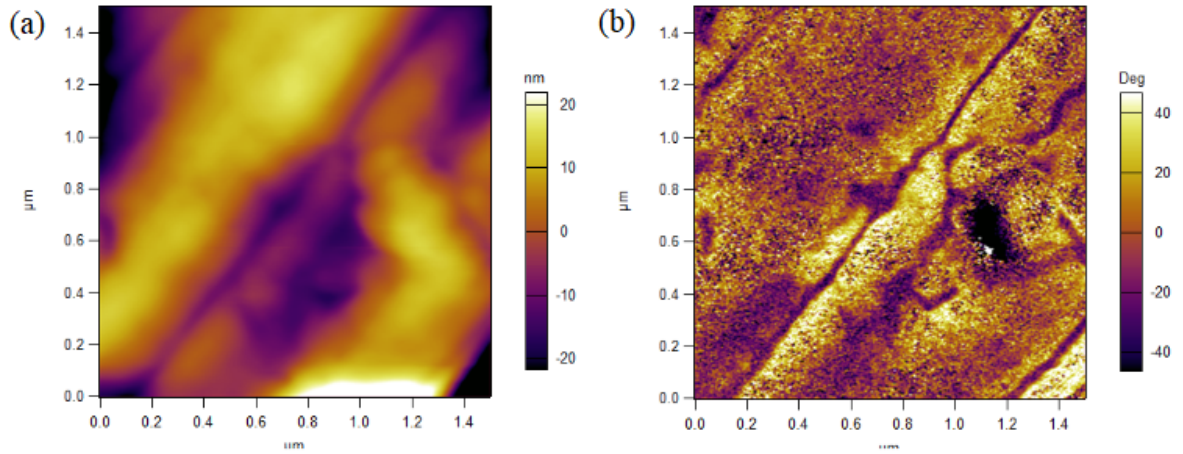

FIGURE 2.4: Topography and phase image for $AgBiTe_2$(1.5μm$\times$1.5μm)

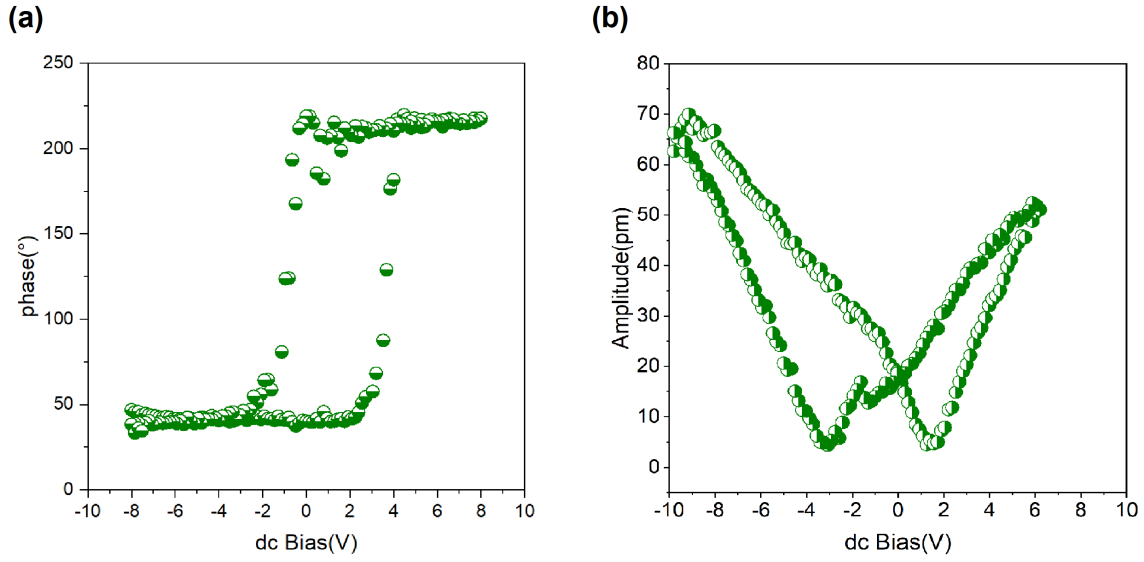

FIGURE 2.5: a) Phase and b) Amplitude of switching spectroscopy PFM(SS-PFM) obtained from rhombohedral $(GeSe)_x(AgBiSe_2)_{1-x}$

polarization and switching behaviour under an externally applied electric field. Spectroscopic measurements were performed by employing switching spectroscopy PFM(SS-PFM) protocol developed by Jesse *et al.,* where a sequence of DC voltage in triangular saw tooth form was applied between the tip and the sample[Jesse, 2006]. This was done to reduce the effects of electrostatic interaction by taking amplitude and phase responses in the off state. The phase of the response signal gives the direction of polarisation while amplitude gives the magnitude of local electromechanical response. In Fig 2.6a and Fig 2.7a, we show hysteresis in phase(ϕ) vs. dc bias plots, which exhibits hysteresis behaviour in phase with nearly 180switching of electrical polarisation. The amplitude of PFM signal

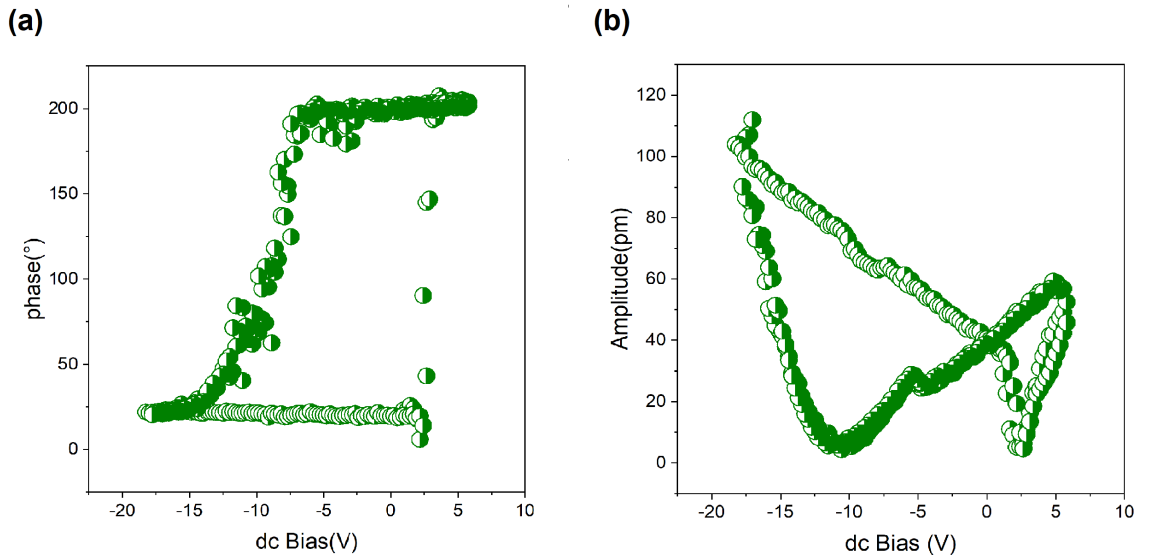

FIGURE 2.6: a) Phase and b) Amplitude of switching spectroscopy PFM(SS-PFM) obtained from rhombohedral $(GeSe)_x(AgBiTe_2)_{1-x}$

is depicted in Fig 2.6b and Fig 2.7b which displays butterfly-shaped loop which further confirms the presence of local ferroelectric domains in both the samples.

2.4 Conclusion

In conclusion, we have performed PFM measurements on GeSe/$AgBiSe_2$ and GeSe/$AgBiTe_2$, where we observed ferroelectric like hysteresis in phase vs.voltage and butterfly loop in amplitude vs.voltage which is a hallmark of ferroelectricity.
Thus, it can be concluded that local ferroelectricity exist in both $(GeSe)_x(AgBiSe_2)_{1-x}$ and $(GeSe)_x(AgBiTe_2)_{1-x}$ which induces ferroelectric instability. This gives rise to low thermal conductivity and high thermoelectric performance in the sample.

Chapter 3

Investigation of magnetic materials using magnetic force microscopy

3.1 Introduction

Magnetic force microscopy has been extensively used to study the magnetic properties of materials at nanoscale due to its high sensitivity and resolution. It has been a well-established method in the characterization of magnetic recording media and superconductors. MFM is another variety of atomic force microscopy where a magnetic tip is scanned across the surface of samples and the magnetic interactions are detected to study the magnetic structure of the sample. It generally measures the interaction between the magnetized tip and stray field emanating from the sample. Mostly a silicon tip with magnetic material is used in tapping mode. The technique is a modification of AFM where the tip is lifted to a certain height and scanned after measuring topography along a single scan line. The force is measured by the shift of phase of cantilever oscillation, where the sign of phase indicates whether the interaction is attractive or repulsive. Here we try to investigate the magnetic structures in two different samples, namely, a CoPt hall bar device and Fe_2O_3 nanoparticles. A CoPt thin film exhibits perpendicular magnetic anisotropy. MFM was employed to study the evolution of magnetic domains in the sample as a function of the applied field. Fe_2O_3 nanoparticles have been reported as material which shows superparamagnetic behaviour with a blocking temperature of 50K[Khalafalla, 1972]. SQUID measurements also confirmed the superparamagnetic behaviour for particles prepared by hydrothermal synthesis

method[Marin Tadica, 2014]. We tried to investigate the presence of any magnetic structures in these nanoparticles which was prepared using a simple precipitation method. Both of these materials have been shown to exhibit magnetic ordering at room temperature.

3.2 Magnetic force microscopy

The magnetic force microscopy is a technique based on atomic force microscopy where a magnetic probe is used to detect the stray fields near the surface of the sample. The principle of operation of MFM is similar to AFM. It can be operated in both contact and tapping mode. However, the most commonly used method involves tapping mode. The cantilever is excited close to its resonant frequency with a certain amplitude and phase. Due to the interaction between the probe and sample the resonant frequency between the sample and tip decreases which leads to a change in oscillation amplitude of the sample. The most widely used detection method involves the usage of the amplitude signal and is termed as amplitude modulation. Another method called frequency modulation technique is more effective in the systems with high Q value. Here the cantilever is made to oscillate directly at its resonant frequency with the help of feedback amplifier with amplitude control[Grütter P, 1992]. The magnetic force acting between the MFM tip is then calculated as

$$\vec{F} = \mu \int \vec{\nabla}(\vec{M_{tip}} \cdot \vec{H_{sample}}) dV_{tip} \tag{3.1}$$

The oppositely magnetised domains in the sample result in the stray field that is detected by the magnetic tip on the sample surface. The presence of opposite magnetic domains in the sample would result in opposite interaction between the tip domain walls. The attractive and repulsive forces cause the cantilever to oscillate differently and give a qualitative understanding of the stray fields in the sample. However such imaging techniques cannot be used to quantify the stray fields in detail.

The technique for imaging the sample involves a dual-pass technique where the sample surface is scanned twice. In the first scan, the intermittent contact mode gives the topography of the sample. For the second scan, the cantilever tip is raised a small distance and scanned along the topography line scanned in the first scan. At this stage, cantilever tip interacts only by magnetic force caused by the stray field. This minimizes the effect caused by other forces[Ferri F A, 2012].

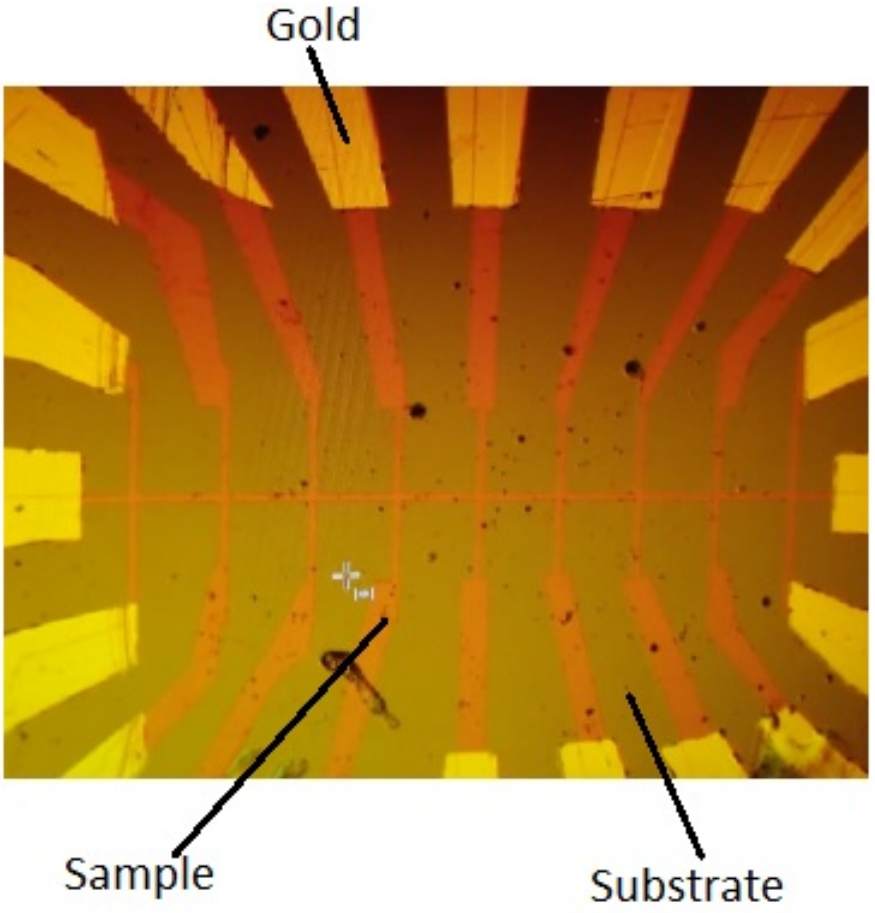

FIGURE 3.1: Co/Pt/Fe Hall bar device

3.3 Experimental Consideration

CoPt hall bar device consisted of a CoPt-Fe thin film heterostructure which was patterned in a hall bar arrangement with gold contacts made using lithographic techniques(Fig 3.2). Magnetic force microscopy was performed on the above sample at different magnetic fields.

Fe_2O_3 nanoparticles were prepared by simple precipitation method. The precursors used were $FeCl_3 \cdot 6H_2O$ and $Liq.NH_3$. Definite Stoichiometric amount of $FeCl_3 \cdot 6H_2O$ was added to deionised water and 12% NH_4OH was added to the above solution. Fe_2O_3 particles were then washed, dried and calcinated at 200C to obtain nanoparticles. Fe_2O_3 nanoparticles obtained was spin-coated onto Si wafer. Magnetic force microscopy was performed on the above nanoparticles to detect any magnetic order.

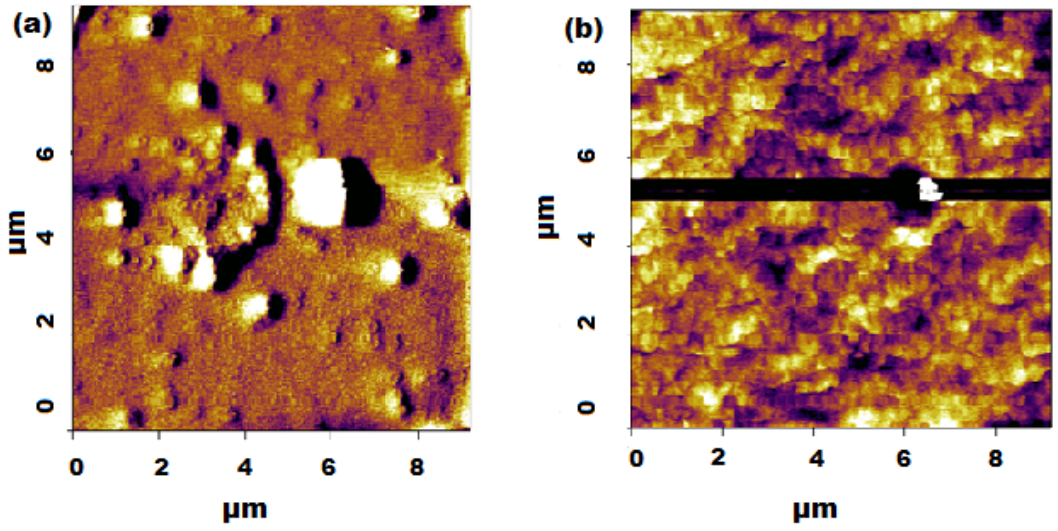

FIGURE 3.2: a) Topography, b) lift mode image of hall bar device(9μm$\times$9μm area)

3.4 Results

The morphology and the magnetic characteristics of CoPt-Fe heterostructures were investigated by AFM and MFM measurements. Topographic data(3.2a) revealed irregularities along the surface of the sample. MFM imaging was performed at different magnetic fields which suggested the presence of magnetic activity in the sample(fig 3.3). It also produced a remarkable contrast in the MFM image. As the magnetic field was changed from 0T to 0.75T the domain structure also evolved.

Fe_2O_3 nanoparticles were imaged using magnetic force microscopy in the absence of any magnetic field. Fig 3.4 shows topography and phase images of nanoparticles. AFM topography was analysed to obtain the size distribution of the particles. The average size of particle ranged between 10-100nm. The contrast in phase images in lift mode is caused by the interaction of the MFM probe and magnetic field from the particles. It suggests the presence of magnetic structures.

3.5 Conclusion

By imaging the Co-Pt hall bar device we were able to analyse the evolution of magnetic domains with the change in the magnetic field. Many of the Co/Pt Iron-based thin films

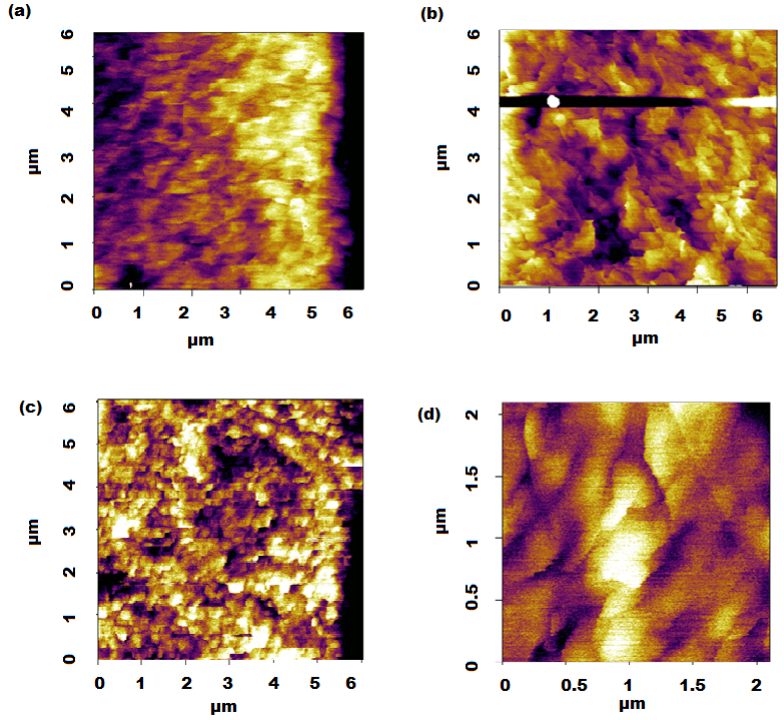

FIGURE 3.3: lift mode image of the Co/Pt/Fe hall bar device of scan size of: (a) 6μm×6μm at magnetic field of 0T, (b) 6μm×6μm at magnetic field of 0.45T, (c) 6μm×6μm at magnetic field of .75T, (d) 2μm×2μm at magnetic field of 0.75T.

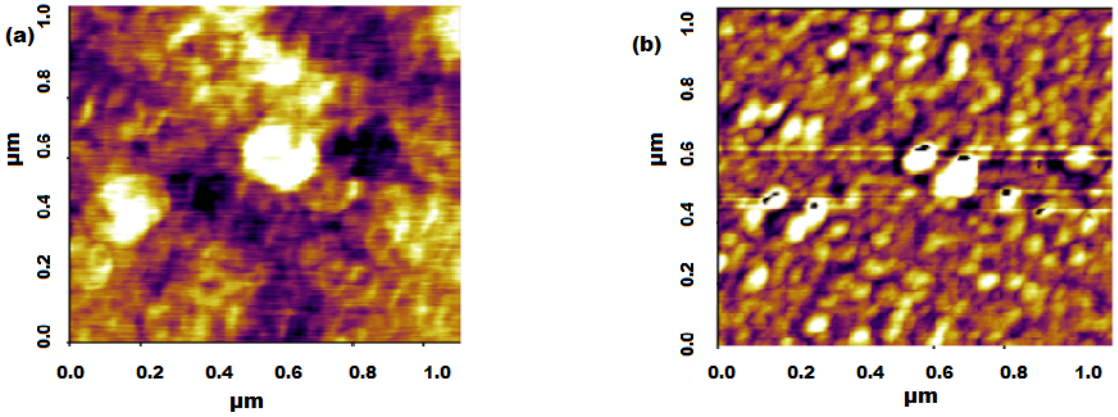

FIGURE 3.4: a) Topography, b) lift mode image of Fe_2O_3 nanoparticles

have been recently known to evolve to topological spin structures termed skyrmions near room temperature. However, we were not able to image any skyrmion formation in the sample. We have also demonstrated that MFM can be used to image and characterize magnetic nanoparticles. Magnetic iron oxide nanoparticles are used in various biomedical applications. The ability of MFM to image these particles at very high resolution has a wide variety of application in optimising its synthesis and characterisation in the different biological environment.

Chapter 4

Magnetic imaging of artificial spin ice system

Since the discovery of spin ice behaviour in $Ho_2Ti_2O_7$ and $Dy_2Ti_2O_7$ several studies were conducted to understand these complex magnetic materials. Artificial spin ice was created to investigate various thermodynamic and magnetic properties associated with these materials, which could be fabricated with precise specifications. It consists of complex nano-sized arrays of ferromagnetic islands arranged on specific lattice fabricated using lithographic techniques. These islands are arranged such that the dipole interactions create a two-dimensional analogue to spin ice. It allows fine control of geometry and to perform the direct investigation using magnetic force microscopy. Here we try to fabricate spin ice made up of permalloy and to characterise them using Magnetic force microscopy.

4.1 Introduction

In geometrically frustrated magnetic materials, the interaction between magnetic degrees of freedom in lattice conflicts with underlying crystal geometry[Roderich Moessner, 2006]. One of the simplest examples of such geometrically frustrated system is an antiferromagnetic triangle where one of the two spins on an elementary triangle are anti-aligned to satisfy antiferromagnetic interaction and the third can no longer point in the direction opposite to either of other spins. Hence it is not possible to energetically minimize all the interaction simultaneously. Such geometric frustration from spins which result from a well-ordered

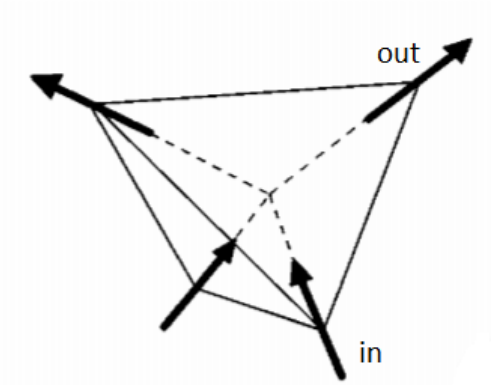

FIGURE 4.1: "two-in/two-out" configuration

structure other than disorder results in a large number of the degenerate manifold of ground states rather than single stable ground state configuration creating a wide range of novel low-temperature behaviour like spin liquid state, frozen states etc. One class of such geometrically frustrated magnetic system is termed as spin ice[Roderich Moessner, 2013].
Spin ice is named in analogous to hydrogen positions in ice, where despite the presence of well-ordered lattice structure, the hydrogen positions are completely disordered. Here the hydrogen atom follows the so-called 'ice rules' which requires that four hydrogen atom surrounding each oxygen atom be placed in tetrahedral coordination where two of them are placed close to the central oxygen atom, while the other two are placed close to neighbouring oxygen atoms. Like the disordered positions in ice, there is a complete disorder in magnetic moment directions in spin ice despite having a well-ordered structure[Isakov S V. and L, 2005].

The spin ice materials have a pyrochlore structure where atoms form a lattice of corner-sharing tetrahedra with spins residing on its sites. Ferromagnetic and dipole interactions cause the spins to align two-in and two-out on each tetrahedron. However, it is difficult to investigate individual spins in material to study how they accommodate frustration of spin interactions without altering the state of the system. Other limitations include the inability to change the geometry and to control defects. Hence in analogy to such systems, artificial spin ice was created which consisted of arrays of single ferromagnetic domains which have intrinsic magnetic moments. With modern developments in lithographic techniques, it is possible to etch out the ferromagnetic films to create nanoislands which are small enough to be single domain. Shape anisotropy gives Ising like spins with the direction which is determined by the shape of the island.[Wang R F, 2006]
They interact mainly through a dipolar magnetic field. Sometimes they can interact via

exchange interactions which are achieved by connecting the islands. One of the main advantages of artificial spin ice is that it can be visualised directly through various imaging techniques. These nanoislands which have lateral dimensions of order 100nm are fabricated using electron beam lithographic techniques. In the case of single-domain ferromagnetic islands, the islands can be placed close to each other and can be arranged in any of the geometric patterns. The relative moment direction in neighbouring islands is influenced by magnetostatic coupling between them[Sandra H Skjærvø1, 2020][Isakov S V. and L, 2005]. In this experiment, we tried to image artificial spin ice which consisted of nanoislands made up of Permalloy which were arranged in four different patterns using electron beam lithography.

4.2 Fabrication and Imaging

We studied nanomagnetic arrays consisting of a two-dimensional square lattice of Permalloy islands on Si wafer with an oxide layer which was fabricated using electron beam lithographic technique. The lithography involves spin-coating the wafer with a resist and exposing it to an electron beam. A mask is used to transfer the design onto the spin-coated resist. Then soluble areas of the resist are then dissolved using a developer chemical by which patterns become visible on the wafer. Then using thermal evaporation technique Permalloy was grown on the pattern which is capped using to prevent oxidation. After the lift-off process using acetone resists are removed and we get Permalloy nanoisland on Si substrate. The nanoislands were then imaged using AFM technique to see the pattern. MFM was performed at zero fields to image the magnetic domains.

4.3 Results

The MFM images of permalloy thin film deposited using thermal evaporation technique is shown in Fig.4.2 which shows striped magnetic domains in the lift mode(Fig 4.2b). The Permalloy was then deposited on the patterned wafer and nano islands were fabricated by lift off technique. The topographic image and height profile of the nano islands kept for lift off for a time period of 1.5 hrs are shown in the Fig 4.3 and Fig 4.4. Nano islands prepared in a similar way but kept for lift-off for a period of 15hrs is shown in the Fig 4.5. The

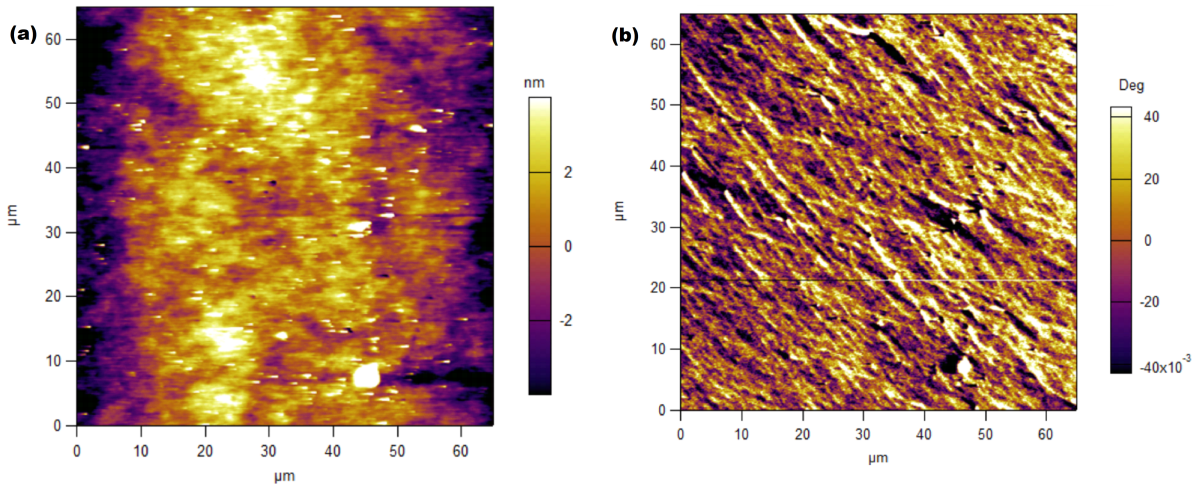

FIGURE 4.2: (a) Topography and (b) lift mode image for Permalloy thin film(65μm×65μm area)

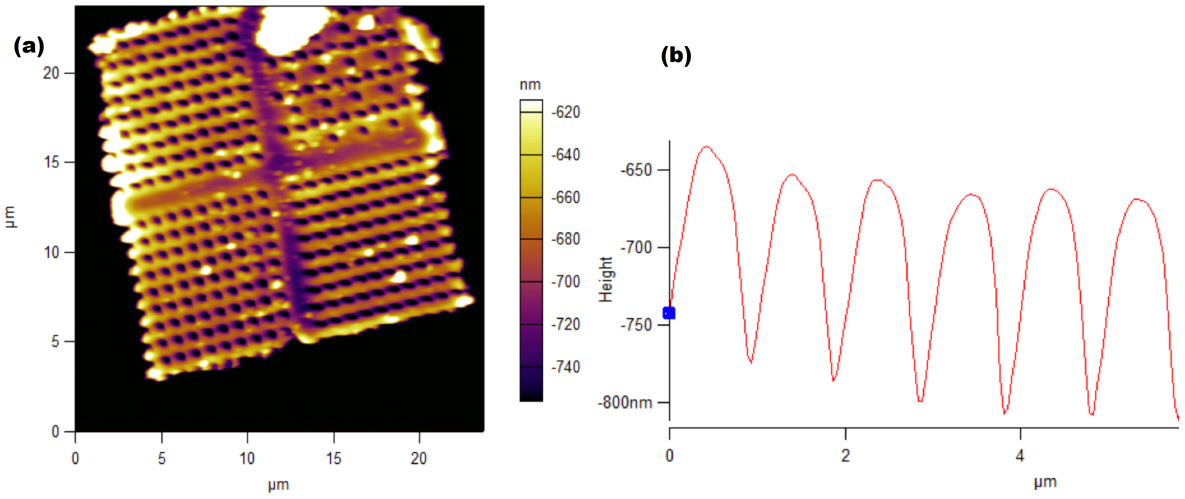

FIGURE 4.3: (a)Topography and (b) Height profile for artificial spin ice(25μm×25μm area,lift-off period 1.5hrs)

magnetic force microscopy of the nano islands was conducted for one of the samples (with lift off period of 1.5 hours) and is shown in Fig 4.6.

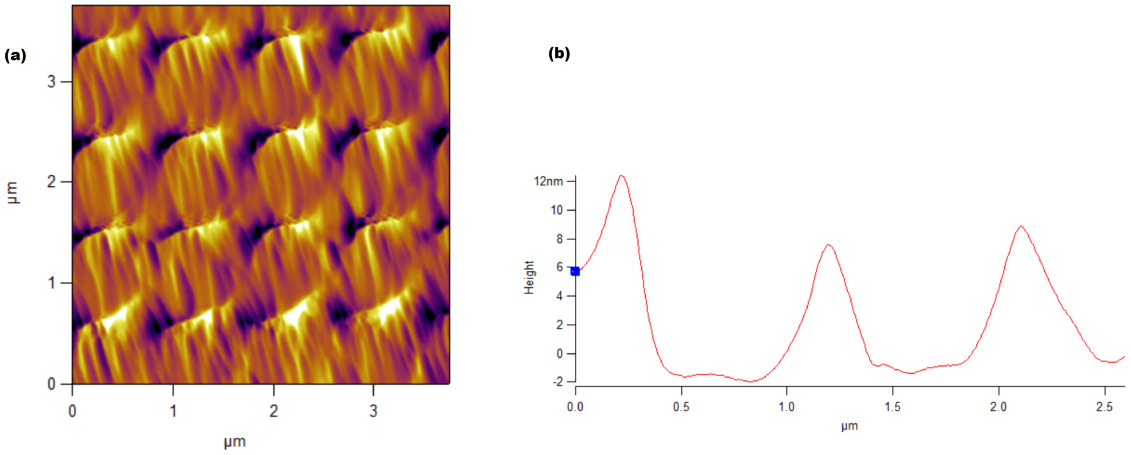

FIGURE 4.4: (a)Topography and (b)Height profile for artificial spin ice(4μm$\times 4\mu$m area, lift-off period 1.5hrs)

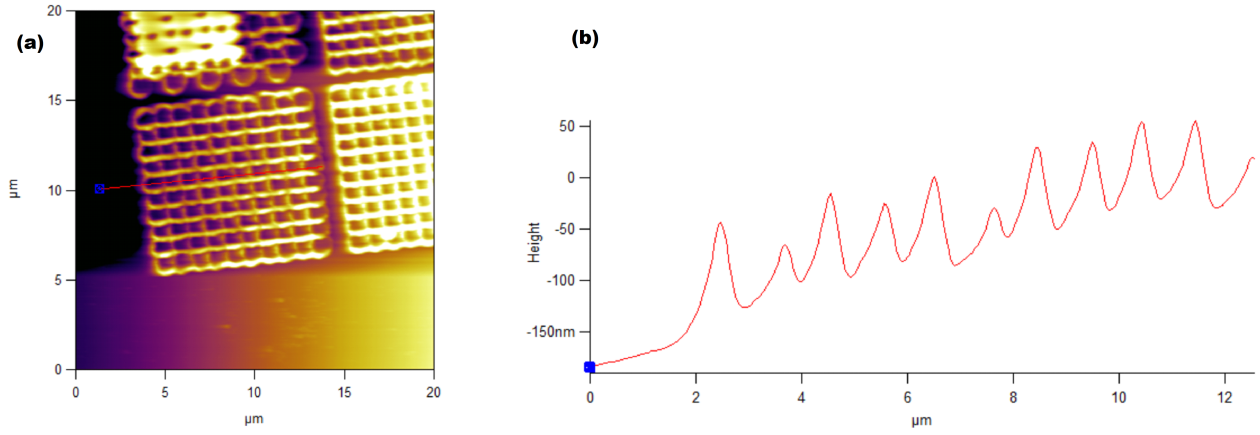

FIGURE 4.5: (a)Topography and (b) Height profile for artificial spin ice(20μm$\times 20\mu$m area, lift-off period 15hrs)

4.4 Conclusion

Most of the researches on artificial spin ice are relatively in the infant stages. Besides being created to mimic the behaviour of spins in crystal counterpart, provides a huge amount of research in itself. Using advanced lithographic and imaging techniques we can fabricate different lattices of magnetic islands and control strength of the interaction. The high-resolution power of magnetic force microscopy helps us in this process. New researches could be done on investigating their dynamics in the magnetic field and measuring entropy to compare with real spin ice.

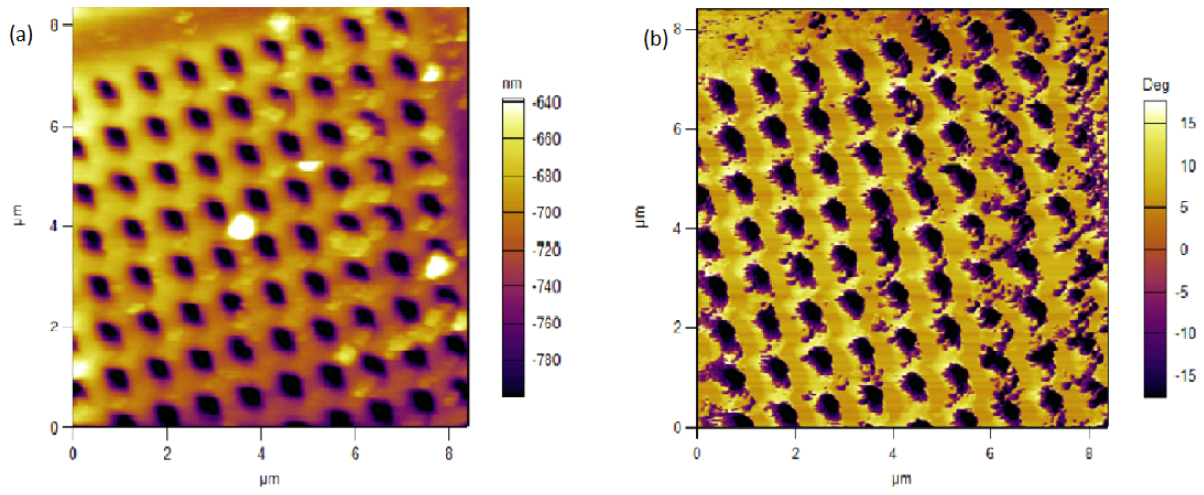

FIGURE 4.6: (a)Topography and (b) Lift mode image for artificial spin ice(8.2μm$\times$8.2μm area, lift-off period 1.5hrs)

Bibliography

[Ferri F A, 2012] Ferri F A, Pereira-da-Silva1 M A, M. J. (2012). Magnetic force microscopy: Basic principles and applications, atomic force microscopy - imaging, measuring and manipulating surfaces at the atomic scale,.

[Giessibl, 2003] Giessibl, F. J. (2003). Advances in atomic force microscopy. *Rev. Mod. Phys.*, 75:949–983.

[Grütter P, 1992] Grütter P, Rugar D, . M. H. J. (1992). Magnetic force microscopy of magnetic materials. *Ultramicroscopy*, 47.

[Huang, 2017] Huang, Z.; Miller, S. A. G. B. Y. M. A. S. W. T. N. P. Z. Y. Z. W. S. G. J. J. P. B. X. (2017). High thermoelectric performance of new rhombohedral phase of gese stabilized through alloying with agsbse$_2$. *Angew. Chem., Int. Ed.*, 56(14113):373.

[Isakov S V. and L, 2005] Isakov S V., M. R. and L, S. S. (2005). Why spin ice obeys the ice rules. *Physical Review Letters*, 95, 217201.

[Jagmeet S Sekhon and Sheet, 2014] Jagmeet S Sekhon, L. A. and Sheet, G. (2014). Voltage induced local hysteretic phase switching in silicon. *Applied Physics Letters*, 104(16).

[Jesse, 2006] Jesse, S.; Baddorf, A. P. K. S. V. (2006). Switching spectroscopy piezoresponse force microscopy of ferroelectric materials. *Appl. Phys. Lett.*, 88(062908).

[Khalafalla, 1972] Khalafalla, J. M. D. C. D. (1972). Superparamagnetic -fe2o3. *physica status solidi.*, 11.

[Marin Tadica, 2014] Marin Tadica, Matjaz Panjanb, V. D. I. M. (2014). Magnetic properties of hematite (-fe2o3) nanoparticles prepared by hydrothermal synthesis method. *Applied Surface Science*.

[Nabil Mahmoud Amer, 1992] Nabil Mahmoud Amer, Armonk N.Y., G. M. (1992). Us pat.re37,299.

[Peter Eaton, 2010] Peter Eaton, P. W. (2010). *Atomic Force Microscopy*. Oxford University Press, Inc., New York.

[Proksch and Kalinin,] Proksch, R. and Kalinin, S. Peizoelectric force microscopy with asylum research afms.

[Roderich Moessner, 2006] Roderich Moessner, A. R. (2006). Geometrical frustration. *Physics Today*, 59,2,24.

[Roderich Moessner, 2013] Roderich Moessner, Cristiano Nisoli, P. S. (2013). Colloquium: Artificial spin ice: Designing and imaging magnetic frustration. *Reviews Of Modern Physics*, 85.

[Roychowdhury, 2017] Roychowdhury, S.; Ghosh, T. A. R. W. U. V. B. K. (2017). Stabilising n-type cubic gese by entropy driven alloying of agbise$_2$; ultralow thermal conductivity and promising thermoelectric performance. *Angew. Chem.*, 56(14113).

[Sandra H Skjærvø1, 2020] Sandra H Skjærvø1, Christopher H Marrows, R. L. S. L. H. (2020). Advances in artificial spin ice. *Nature Reviews*, 2.

[Wang R F, 2006] Wang R F, Nisoli C, F. R. L. J. M. W. C. B. J. (2006). Artificial 'spin ice' in a geometrically frustrated lattice of nanoscale ferromagnetic islands. *Nature*, 439, 303-306.

[Yongho Seo, 2008] Yongho Seo, Wonho Jhe, . (2008). Atomic force microscopy and spectroscopy. *Rep.Prog.Phys*, 71(9).